Supplemental Figure Legends

Supplemental Figure 1. VEGF-A level and vascularity are reduced in the adipose tissue of diet-induced obese mice. A, The body weight of wild-type mice fed a NC or a HFHS diet (*n*=6) (NC; 27.75±1.4g, HFHS; 38.5±2.1g). **B,** GTT and ITT of mice described in **A**. **C,** BAT/body weight ratio (%) of mice described in **A** (*n*=3-9). **D,** Vascularity of BAT evaluated with isolectin IB4 staining (red). Scale bar = 50 μm. The right graphs show vessel number/ adipocyte or vessel number/microscopic field (x400, *n*=4). **E-H,** Levels of VEGF-A evaluated with immunofluorescence and ELISA in BAT **(E** and **F**, *n*=4**),** and WAT **(G** and **H,** *n*=4-5). Scale bar = 50 μm. The right graphs in **E** and **G** show the relative VEGF-A expression area. Data were analyzed by two-tailed Student's *t*-test (**A, C, E-H**) or ANOVA (**B, D**). **P*<0.05, ***P*<0.01. All values represent the mean ± s.e.m.

Supplemental Figure 2. Temporal changes in VEGF-A and mitochondrial markers in BAT of dietary obese model. A, Body weight and BAT/body weight ratio (%) (*n*=6-11), and **B**, hematoxylin and eosin staining of brown adipose tissue (BAT) from a NC- or a HFHS-fed mice maintained on these diets for 1 (1w) or 4 (4w) weeks. Scale bar=50 μm. Right graph shows the number of large lipid droplets/microscopic field in BAT (x400, *n*=4) under these conditions. **C,** Vascularity of BAT evaluated with isolectin IB4 staining at different time points on HFHS diet. The graph shows relative vessel number/microscopic field (x400, *n*=4). **D**, VEGF-A level evaluated by quantitative immunofluorescence staining (*n*=4) **E**, Real-time PCR analysis of *Vegfa* and *Kdr* expression in BAT from a NC or a HFHS fed mice maintained on these diet for 1 (1w) or 4 (4w) weeks (*n*=4-10). **F,** Pimonidazole staining in BAT determined by Hypoxyprobe-1 staining. The right graph indicates the pimonidazole positive area (*n*=4). ND indicates not

detected by pimonidazole staining. Scale bar=50 μm. **G**, Real-time PCR analysis of mitochondrial marker expression in BAT (*n*=4-11). For this experiment, the HFHS fed mice (1w, 4w) (**C,D,E,G**) were compared with NC fed mice (1w, 4w), respectively. Data were analyzed by two-tailed Student's *t*-test (**A-G**). **P*<0.05, ***P*<0.01. All values represent the mean ± s.e.m. NS = not significant.

Supplemental Figure 3. VEGF-A level and vascularity are reduced in the ob/ob genetic model of obesity A, Body weight and BAT/body weight ratio (%) of WT vs. ob/ob mice (*n*=5-7). **B**, Hematoxylin and eosin staining of brown adipose tissue (BAT) or white adipose tissue (WAT) from ob/ob and littermate control (WT) mice. Scale bar=50 μm. Right graph shows the number of large lipid droplets/field in BAT (x400, *n*=3-4) **C,** Vascularity of BAT evaluated with isolectin IB4 staining. The graph shows vessel number/field (x400, *n*=4). **D,** Pimonidazole staining in BAT and WAT of ob/ob and littermate control (WT) mice estimated by Hypoxyprobe-1. The right graph indicates the pimonidazole positive area (*n*=4). Scale bar=50 μm. **E,** Western blot analysis of VEGF-A in BAT from WT and ob/ob mice. The right graph indicates the quantification normalized to GAPDH expression (*n*=3). **F**, VEGF-A level in BAT and WAT evaluated with the immunofluorescent staining (*n*=3-4) **G**, Real-time PCR expression of *Vegfa* and *Kdr* in BAT and WAT of WT and ob/ob mice (*n*=7-8). **H**, Real-time PCR expression of mitochondrial markers in BAT of WT and ob/ob mice (*n*=7-8). **I**, Acute cold tolerance test of ob/ob mice and littermate control (WT) (*n*=4). Data were analyzed by two-tailed Student's *t*-test (**A,B,E,F,H**) or ANOVA (**C, D, G, I**). **P*<0.05, ***P*<0.01. All values represent the mean ± s.e.m.

Supplemental Figure 4. VEGF-A level and vascularity are reduced in the adipose tissue of aP2-Cre$^{+/-}$ *Vegfa*$^{flox/flox}$ mice. A, B, Body weight and food intake of aP2-Cre$^{+/-}$ *Vegfa*$^{flox/flox}$ (KO) and wild-type littermates (*n*=4-6). **C-F,** Assessment of VEGF-A in BAT and WAT using immunofluorescence (**C, E)** and ELISA (**D, F)** (*n*=4, scale bar= 50 μm). The right graphs in **C** and **E** show the relative immunofluorescence area of VEGF-A staining. **G,** Vascularity of BAT and WAT from mice prepared in **A** evaluated with staining for isolectin IB4 conjugates (red). Scale bar = 50 μm. The right graph shows vessel number/field (x400, *n*=4). **H,** Pimonidazole staining in BAT estimated by Hypoxyprobe-1. The graph indicates the pimonidazole positive area (*n*=4-7). **I,** Adipocyte size in WAT measured with hematoxylin and eosin staining as shown in Fig. 2D. Two hundred adipocytes were randomly selected for the measurement (*n*=4). **J,** WAT/body weight ratio of mice prepared in **A** (*n*=5-6). **K,** Gross morphology of BAT. **L,** BAT/body weight ratio of mice described in **A** (*n*=4-5). **M,** Number of large lipid droplets/field (x400, *n*=4) measured with BAT prepared in Fig. 2D. Data were analyzed by two-tailed Student's *t*-test (**A-F, H-J, L, M**) or ANOVA (**G**). **P*<0.05, ***P*<0.01. All values represent the mean ± s.e.m.

Supplemental Figure 5. BAT-specific delivery of Vegfa by adenovirus injection. A, Immunohistochemical detection of β-galactosidase in BAT injected with PBS or ad-*LacZ* two weeks prior to obtaining the samples. The right graph demonstrates the ratio of β-gal positive nuclear (n=4)**.** Four fields were randomly selected from each sample for 4 samples. **B,** Western blot analysis of Myc-tagged VEGF-A in BAT of mice injected with ad-*lacZ* (Con) or ad-*Vegfa* (Vegfa) one week prior to obtaining the sample. The right graph shows quantification of VEGF-A expression (*n*=3). **C,** isolectin IB4 staining was performed to assess the vascularity in the BAT

of mice fed NC and HFHS diets, as described in Fig. 3A. Scale bar = 50 μm. **D,** The graph shows vessel number/field (x400, *n*=4) of isolectin IB4 staining shown in **C**. Data were analyzed by two-tailed Student's *t*-test (**A, B**) or ANOVA (**D**). **P*<0.05, ***P*<0.01. All values represent the mean ± s.e.m.

Supplemental Figure 6. Analysis of Vegfa delivery to BAT. A, Immunofluorescence analysis of vessel leakage evaluated with FITC-CM-Dextran in BAT of mice 2 weeks after the injection of ad-*Vegfa* (Vegfa) or a control adenoviral vector (Con) into BAT. Lipopolysaccharides (LPS) was used as a positive control. Scale bar = 50 μm. The right graph indicates FITC positive area per field (x200, *n*=3-4). **B, H,** Real-time PCR analysis of *Emr1, Tnf* and *Ccl2* in BAT (**B**) (compared in NC-fed mice) or WAT (**H**) from mice described in Fig. 3A (*n*=3-6). **C,** Plasma VEGF-A expression evaluated with ELISA in mice (*n*=16-17). **D,** Western blot analysis of VEGF-A transgene and Myc-Tag in WAT of mice described in Fig. 3A. Under the probe conditions, endogenous VEGF-A levels in WAT could not be determined. HEK293 cells infected with ad-*lacZ* (Con) or ad-*Vegfa* (Vegfa) were used as controls, respectively. **E**, Immunofluorescent staining for detecting vessels (Isolectin IB4, green) and adipocytes (Bodipy-TR, red) in WAT of mice described in Fig. 3A. Scale bar = 100 μm. **F**, The graph shows vessel number/field (x400, *n*=4) of isolectin IB4 staining for WAT described in Supplemental Fig. 5C (*n*=4). **G**, Hematoxylin and eosin staining of WAT from mice prepared in Fig. 3A. Scale bar = 50 μm. **I-K,** WAT weight (**I**), Body weight (**J**) and food intake (**K**) of mice prepared in Figure 3A (*n*=3-11). Data were analyzed by two-tailed Student's *t*-test (**B, C, K**) or ANOVA (**A, F, H-J**). **P*<0.05, ***P*<0.01. All values represent the mean ± s.e.m.

Supplemental Figure 7. Vegfa delivery prevents the whitening of BAT and improves glucose metabolism in aP2-Cre$^{+/-}$ *Vegfa*$^{flox/flox}$ mice. The BAT of aP2-Cre$^{+/-}$ *Vegfa*$^{flox/flox}$ (KO) and wild-type mice (WT) injected with ad-*lacZ* (Con) or ad-*Vegfa* (Vegfa), three weeks prior to obtaining the samples. **A,** Western blot analysis of VEGF expression in BAT. The graph below shows quantification of VEGF-A expression (*n*=3). **B**, Immunofluorescent staining for vessel detection (Isolectin IB4, green) and adipocytes (Bodipy-TR, red) in BAT from aP2-Cre$^{+/-}$ *Vegfa*$^{flox/flox}$ (KO) and wild-type mice after the injection of ad-*Vegfa* (Vegfa) or control (Con) adenovirus. Scale bar = 100 μm. **C,** Real-time PCR analysis of *Kdr* expression in BAT of mice (*n*=3-10). **D,** Hematoxylin and eosin staining of BAT from WT and KO mice injected with ad-*Vegfa* or control. Scale bar=50 μm. Right graph shows the number of large lipid droplets/field (*n*=4) **E,** Real-time PCR analysis of *ND5, Ndufa* and *Ppargc1a* expression in BAT of the different experiments sets of mice (*n*=3-10). **F**, Acute cold tolerance test for the different experimental sets of mice (*n*=3-4). **G,** GTT and ITT (*n*=3-11) and **H, I,** WAT weight (**H**) and body weight (**I**) (*n*=4-7) of the different experimental sets of mice. Data were analyzed by ANOVA (**A, C, D-I**). **P*<0.05, ***P*<0.01. All values represent the mean ± s.e.m.

Supplemental Figure 8. Mitochondrial dysfunction and autophagic responses in BAT from obese and VEGF-deficient mice. A, C, Relative quantification of MitoSOX (**A**) or MitoRed (**C**) labeling in isolated mitochondria extracted from BAT of NC- or HFHS-fed mice described in Fig. 4A,B (*n*=4-5). **B, D,** FACS analysis of isolated mitochondria extracted from BAT of aP2-Cre$^{+/-}$ *Vegfa*$^{flox/flox}$ (KO) and wild-type mice (WT). Mitochondrial labeling was carried out with MitoSOX (**B**) or MitoRed (**D**). The right graphs show the relative quantification (*n*=3-5). **E,** Immunofluorescence staining for mitochondrial membrane protein Tom20 (green) and

autophagosomal membrane protein LC3 (red) at x3000 magnification in BAT from aP2-Cre$^{+/-}$ *Vegfa*$^{flox/flox}$ (KO) mice. Arrows show double stained puncta. Scale bar = 3 μm. Right graph shows the frequency of puncta double-stained with Tom20 and LC3 measured on 10 random fields (observed at x3000 magnification, *n*=3). **F,** Real-time PCR analysis of *Bnip3* and *Map1lc3b* expression in BAT of mice prepared in WT and KO mice (*n*=4-5). **G,** Quantification of immunofluorescence staining showing the numbers of puncta of Tom20 co-localizing with autophagosomal membrane protein LC3 in BAT from WT and KO mice whose BAT were injected with ad-*Lacz* (Con) or ad-*Vegfa* (Vegfa). The puncta were measured on 10 random fields observed at x3000 magnification (*n*=4-5). **H,** Real-time PCR analysis of *Bnip3* and *Map1lc3b* expression in BAT (*n*=4-7). Data were analyzed by two-tailed Student's *t*-test (**A-F**) or ANOVA (**G, H**). **P*<0.05, ***P*<0.01. All values represent the mean ± s.e.m.

Supplemental Figure 9. ROS production and autophagic activity are increased in brown adipocytes during hypoxic stress ex vivo and in vitro. A-E, Analysis of BAT cultured *ex vivo* under normoxic and hypoxic conditions (1% O_2 for 12 hr unless otherwise mentioned). **A, B**, FACS analysis for isolated mitochondria extracted from BAT of wild type mice that were cultured *ex vivo* under normoxic or hypoxic (6 hr) conditions and stained with MitoSOX (**A**) and MitoRed (**B**). The graphs at right show the relative quantification (*n*=3-4). **C,** Quantitative analysis of western blots measuring levels of LC3A/B-II expression (*n*=3). **D, E,** Real-time PCR analysis under 12hr (**D**) or 24 hr (**E**) hypoxic stress (*n*=3). **F-M**, Analysis of the cultured brown adipocyte cell line under normoxic and hypoxic conditions (1% O_2 for 12 hr unless otherwise mentioned). **F, G,** Immunofluorescence staining under normoxic or hypoxic (1% O_2 for 6 hr) conditions. **F,** MitoSOX positive mitochondria are indicated by white arrows. The right graph

shows quantification of MitoSOX-positive puncta (*n*=3-4). Scale bar = 10 μm. **G**, Relative staining of functional mitochondria (MitoRed) and total mitochondria (Mito Tracker Green FM (MitoGreen)). Scale bar = 10 μm. **H,** The graph shows quantification of MitoRed positive area in **G** (*n*=3-4). **I,** Quantification of Western blot analysis of LC3A/B-II expression (*n*=3). **J,** Immunofluorescent staining showing mitochondrial membrane protein Tom20 (green) co-localizing with autophagosomal membrane protein LC3 (red). Scale bar = 3 μm. **K,** The graph shows the numbers of puncta double stained with Tom20 and LC3 for **J** (*n*=3-4). **L, M,** Real-time PCR analysis under 24hr hypoxic stress (*n*=4-5). Data were analyzed by two-tailed Student's *t*-test. **P*<0.05, ***P*<0.01. All values represent the mean ± s.e.m.

Supplemental Figure 10. Hypoxia induced Hif1a expression does not contribute to VEGF induction. A, B, Immunohistochemical staining for Hif1a expression in BAT and WAT of NC- or HFHS-fed mice (**A**) or the brown adipocyte cell line cultured under normoxic and hypoxic conditions (1% O_2 for 24 hr) (**B**). The right graph indicates the degree of Hif1α induction (*n*=3-8). Scale bar = 50 μm. **C-F**, Real-time PCR analysis of *Hif1a, Vegfa, Bnip3* and *ND5* expression in differentiated brown adipocyte line transduced with ad-*Hif1a* (Hif1a) or a control adenoviral vector (Con) for 48 hr (*n*=3-6). **G-K**, Real-time PCR analysis of *Hif1a, Vegfa, Bnip3, ND5, Eln* and *Lox* expression in BAT of WT, NC-fed mice injected with ad-*Hif1a* (Hif1a) or a control adenoviral vector (Con) 2 weeks prior to obtaining samples (*n*=4-10). **L**, Real-time PCR analysis of *Eln* and *Lox* in BAT from mice fed NC or HFHS diet (*n*=7). Data were analyzed by two-tailed Student's *t*-test (**B-L**) or ANOVA (**A**). **P*<0.05, ***P*<0.01. All values represent the mean ± s.e.m.

Supplemental Figure 11. Regulation of VEGF-A and Adrb1 and Adrb3 expression. A,**B**, ELISA measurement of FFA in BAT (*n*=4) of mice fed a NC or a HFHS diet for 8 or 1 week. **C-K**, Analysis of the cultured brown adipocyte cell line treated with palmitic acid (500 μM for 48 hr) or normoxic and hypoxic stress (1% O_2 for 24 hr unless otherwise mentioned). **C, D,** VEGF-A level as evaluated by western blot analysis (**C**) or real-time PCR (**D**) (*n*=4). The western blot was normalized to tubulin expression (*n*=3). **E,** Real-time PCR analysis of *Adrb1* and *Adrb3* expression (*n*=5-7). **F, G, J,** Western blot analysis of the ADRB1 (**F**), ADRB3 (**G**) and pPKA (**J**). The right graphs indicate the quantification expression of ADRB1 and 3 relative to GAPDH loading control or pPKA relative to PKA (n=3). **H, I,** Radioligand binding assay showing the reduced level of β1 and β3-adrenergic receptor under hypoxic condition. [^{3}H]-(-)-CGP-12177 was used at a concentration of 0.1-2.5nM when examining the high-affinity β1-adrenoreceptor site (**H**) and 0.1-100nM for the low-affinity β3-adrenoreceptor site (**I**). β1-adrenoreceptor antagonist CGP20712A (10μM), β3-adrenoreceptor antagonist SR59230A (10μM) was used respectively to define specific binding (n=8-9). **J,** Western blot analysis of phosphorylated protein kinase A (pPKA Thr197) and total PKA. The right graphs indicate the quantification expression of pPKA relative to PKA (n=3). **K,** ELISA measurement of cAMP (n=3-6). Cells were treated with 0.1-100 μM isoprenaline hydrochloride (ISO) for 20min. Data were analyzed by two-tailed Student's *t*-test (**A-G, J, K**) or ANOVA (**H, I**). **P*<0.05, ***P*<0.01. All values represent the mean ± s.e.m.

Supplemental Figure 1

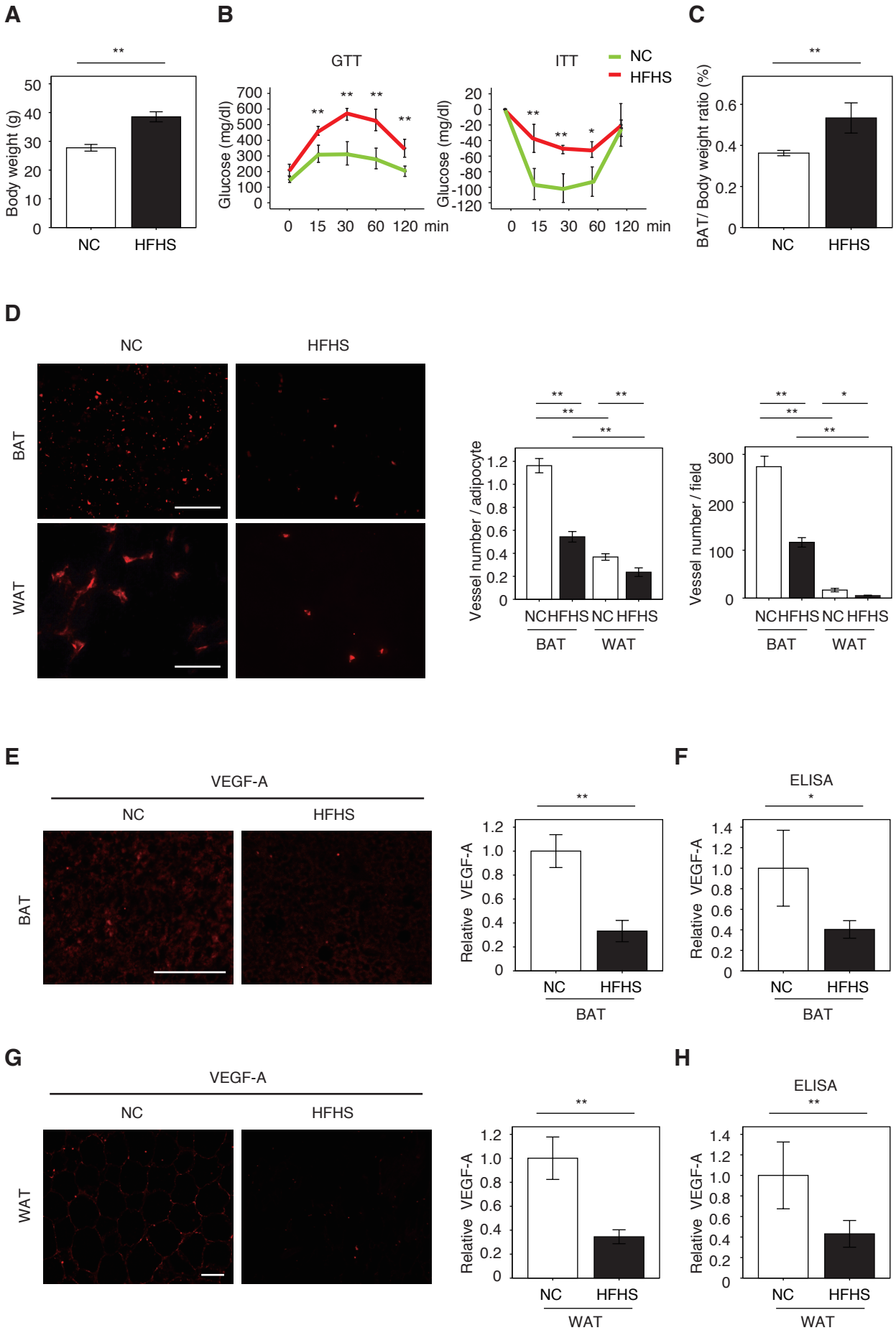

Supplemental Figure 2

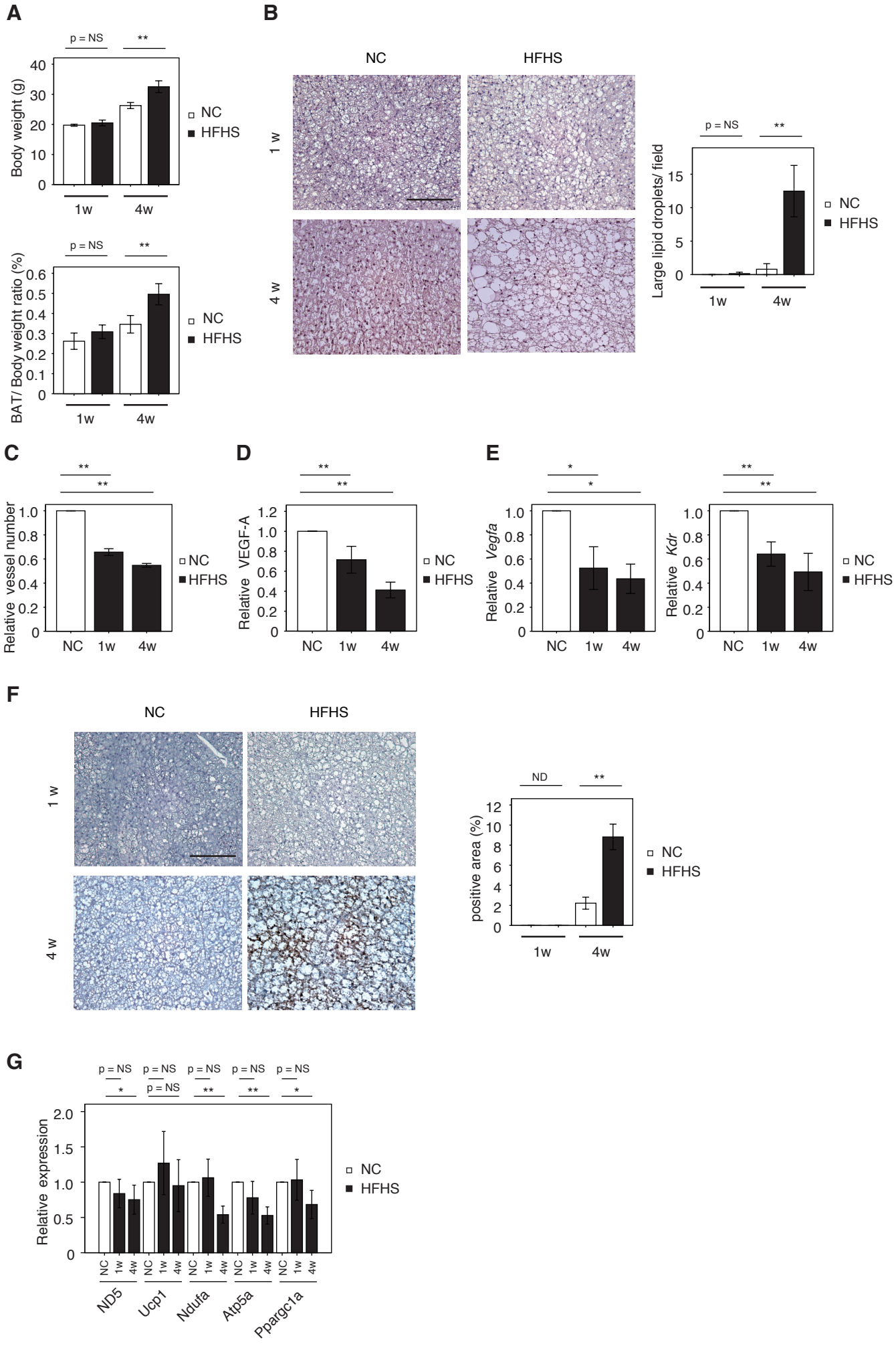

Supplemental Figure 3

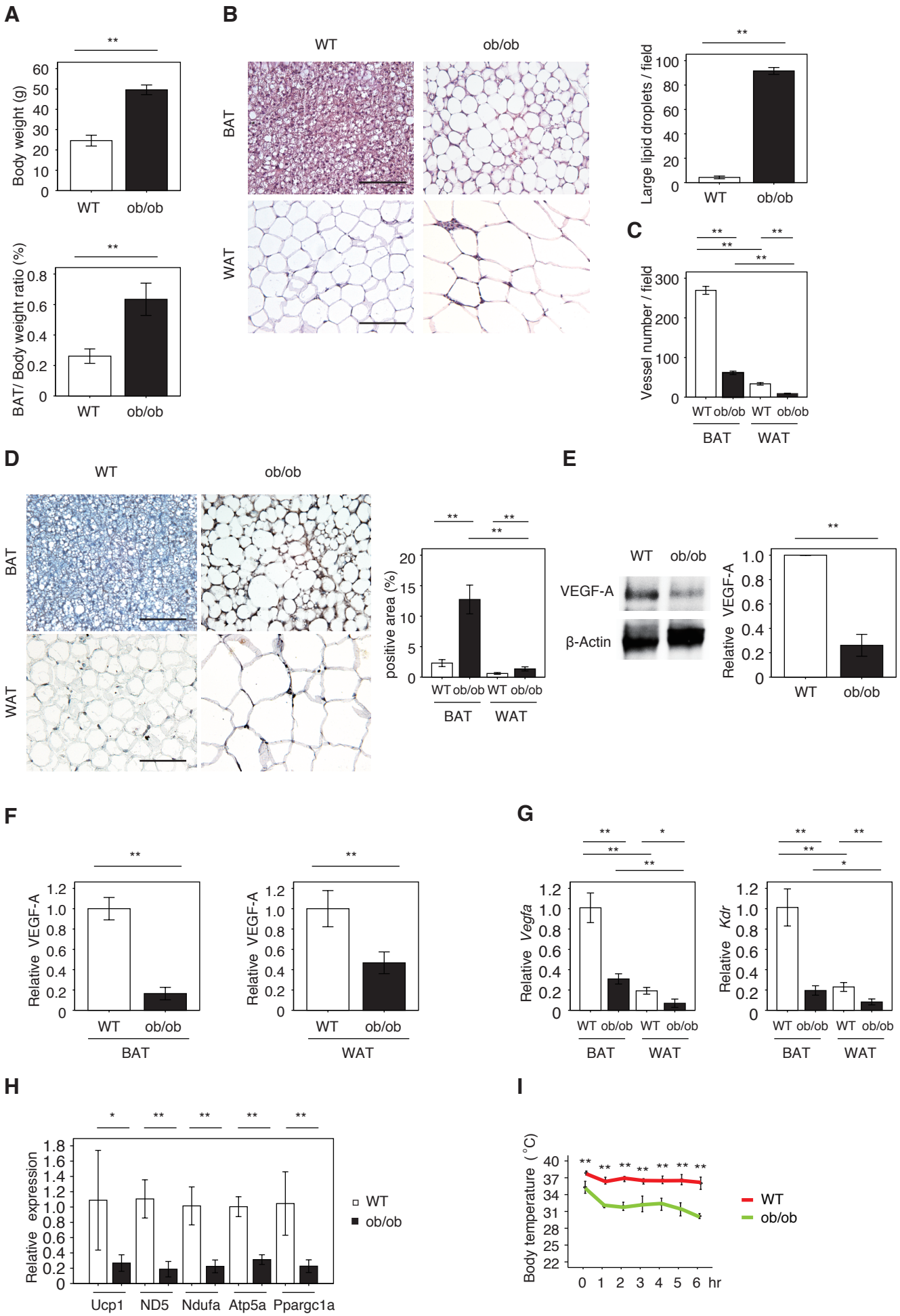

Supplemental Figure 4

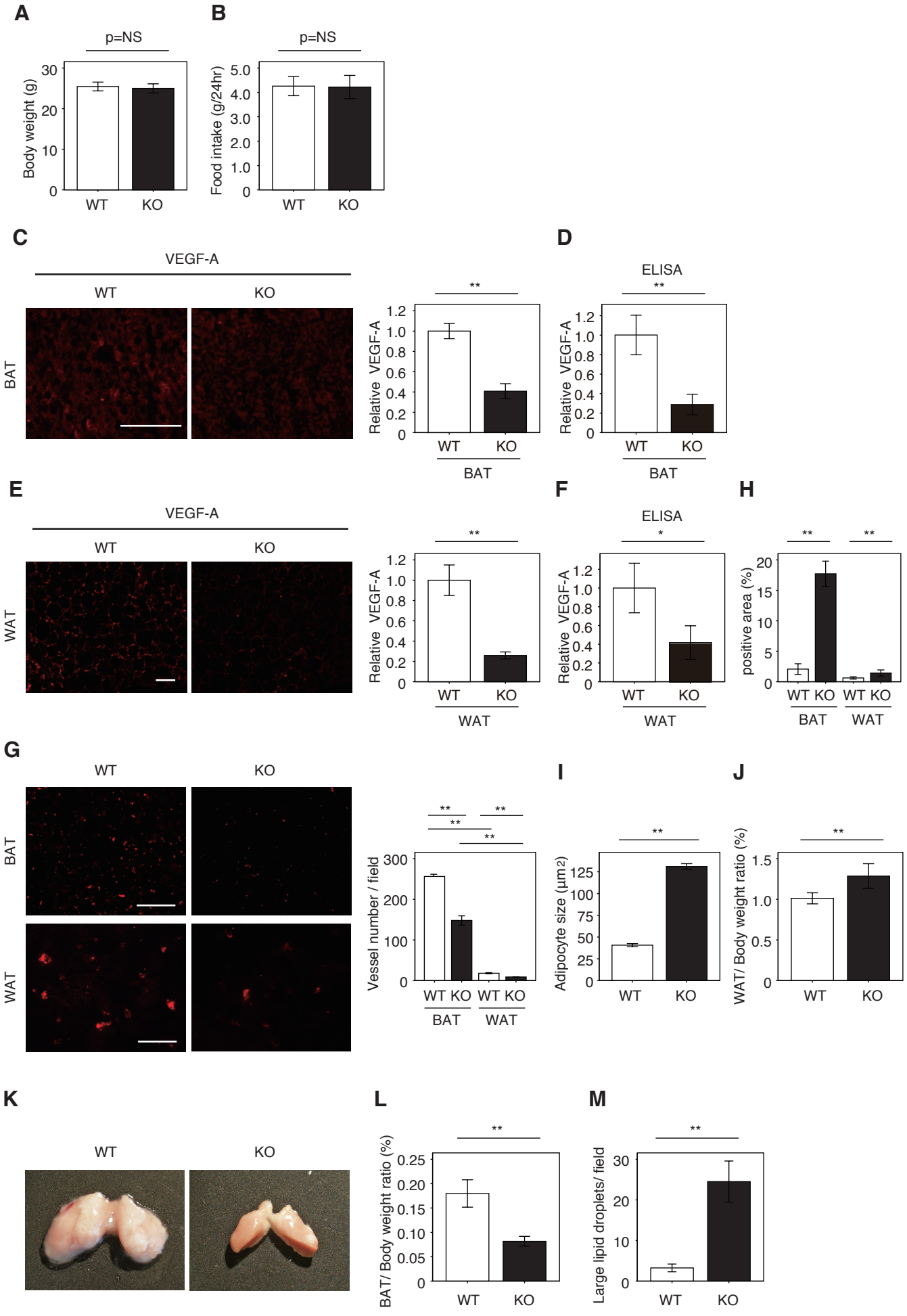

Supplemental Figure 5

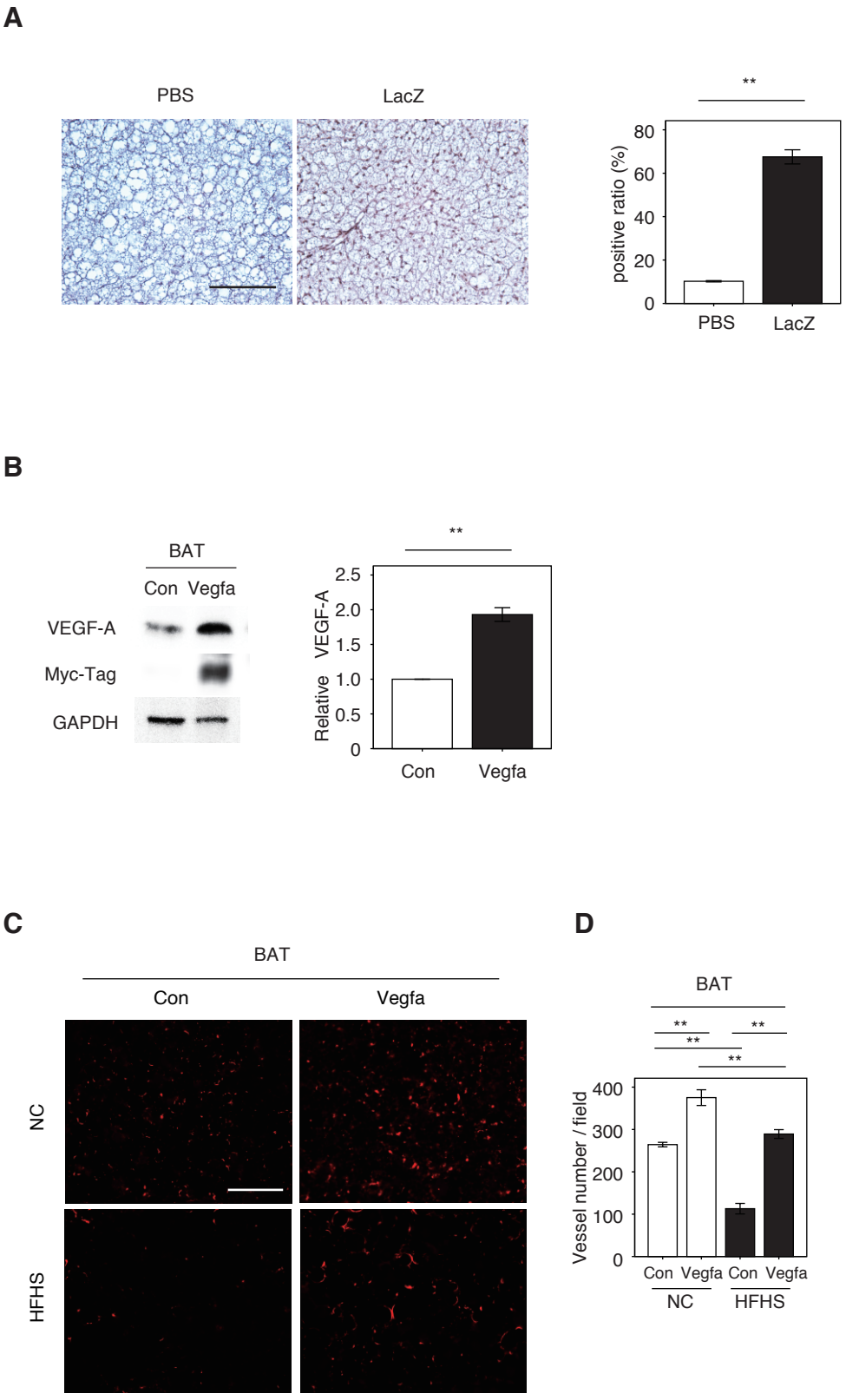

Supplemental Figure 6

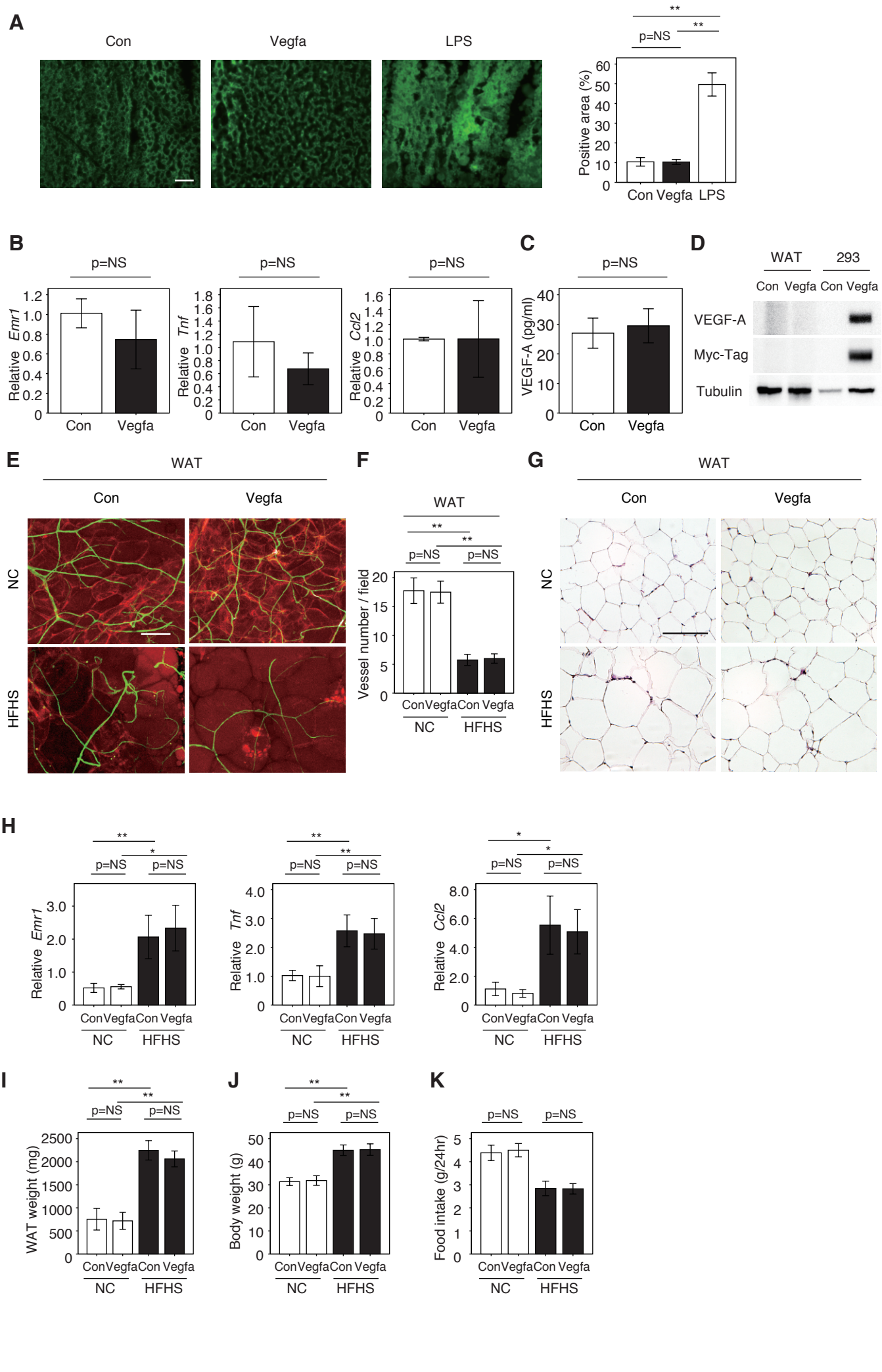

Supplemental Figure 7

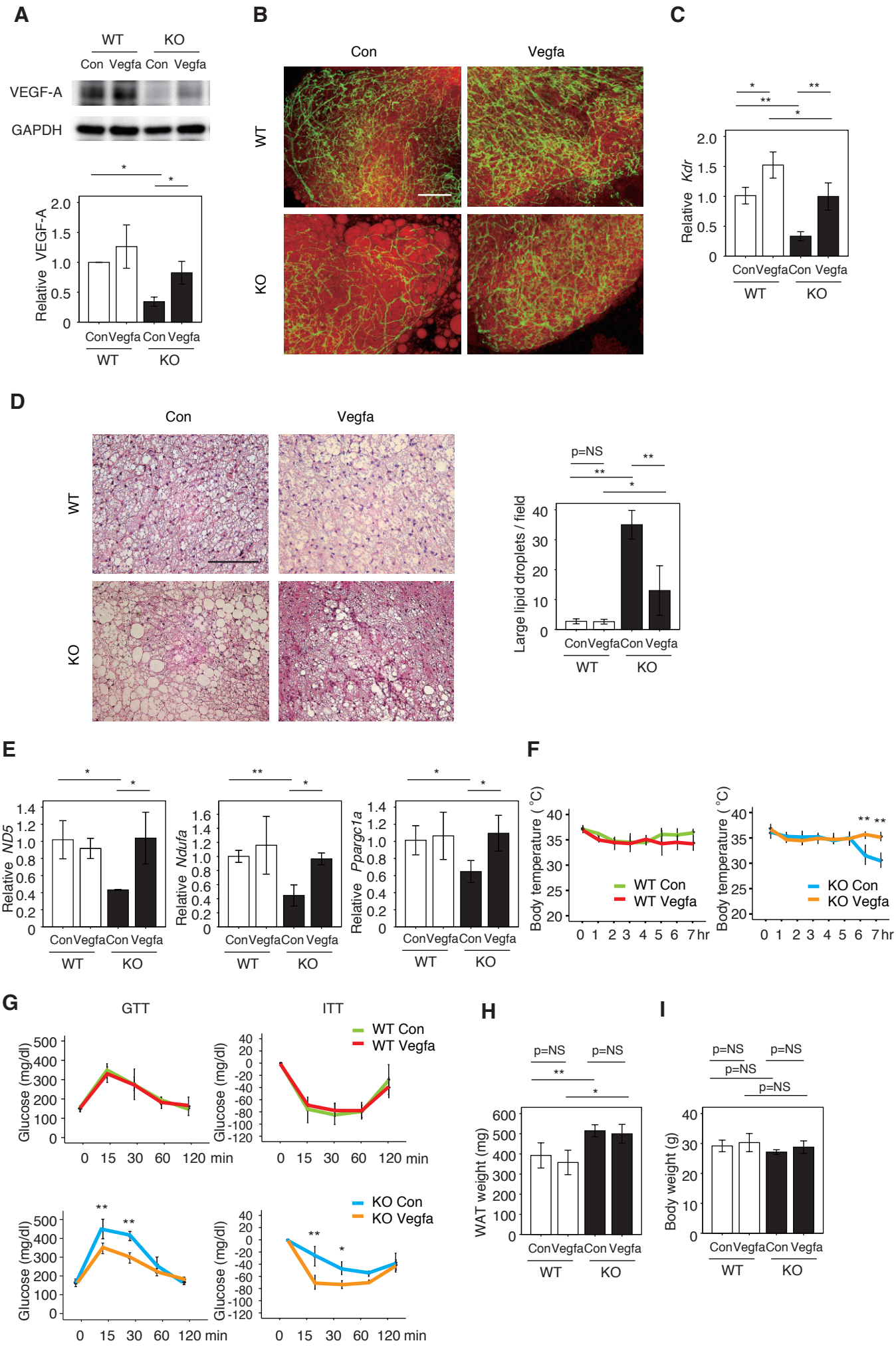

Supplemental Figure 8

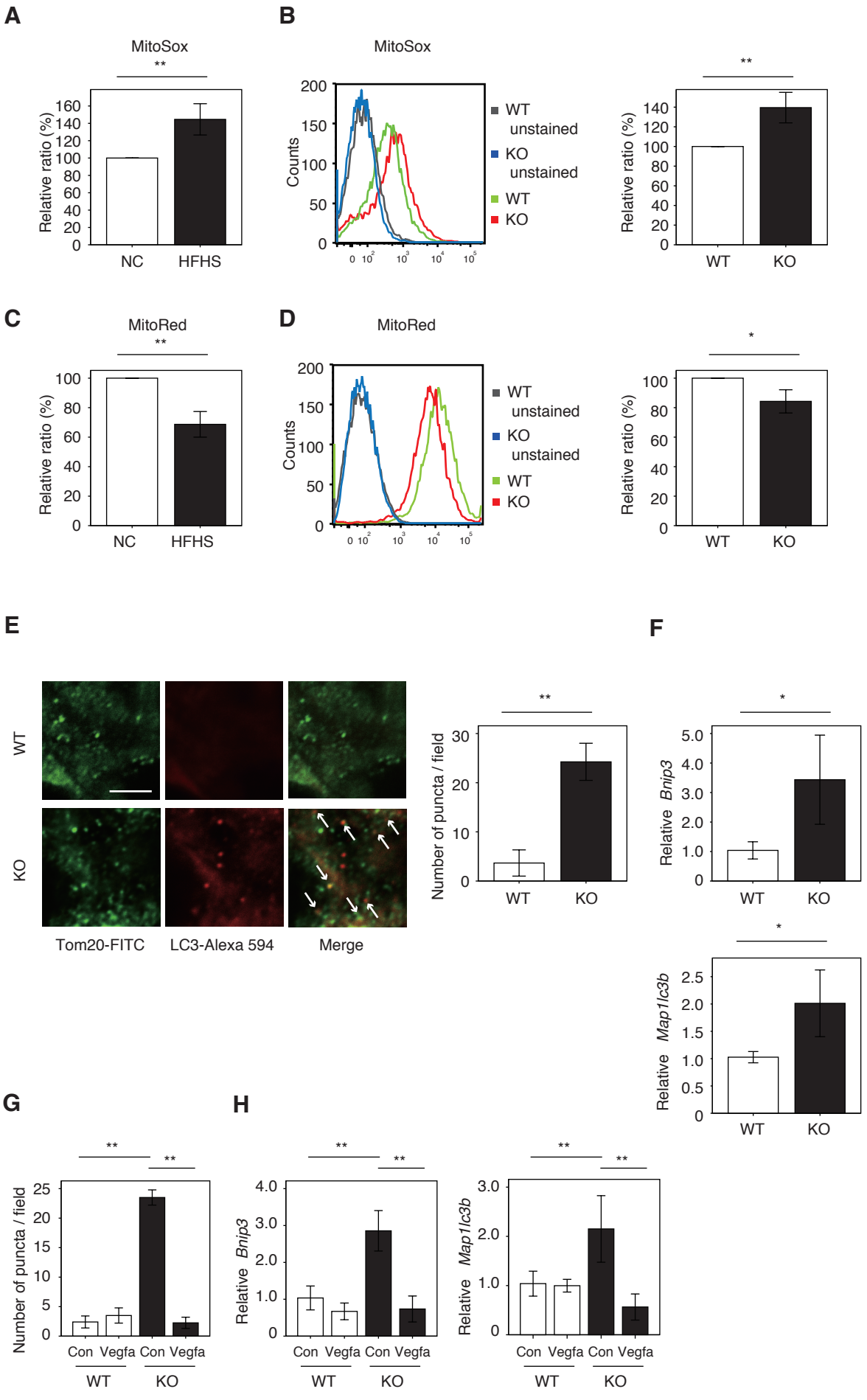

Supplemental Figure 9

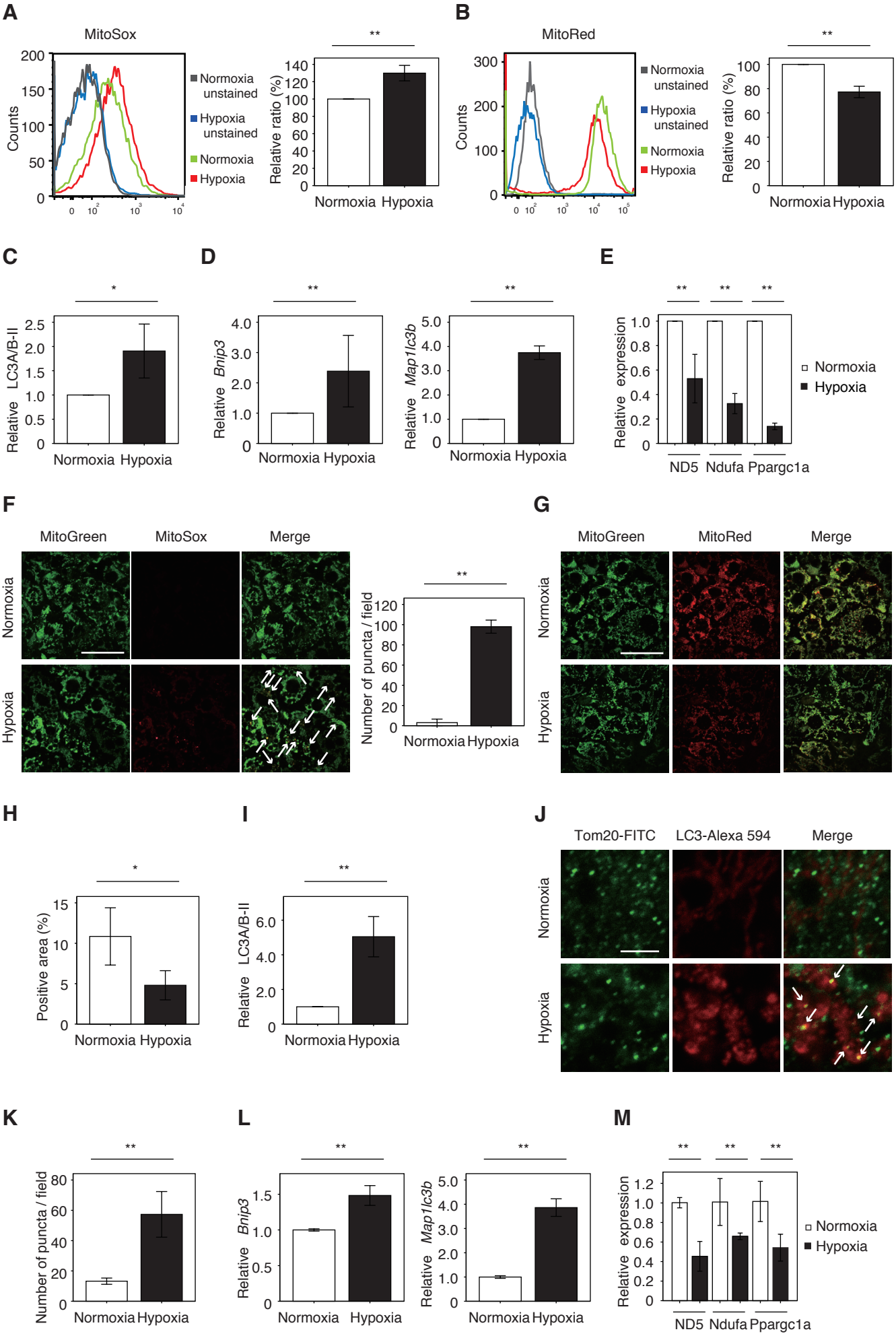

Supplemental Figure 10

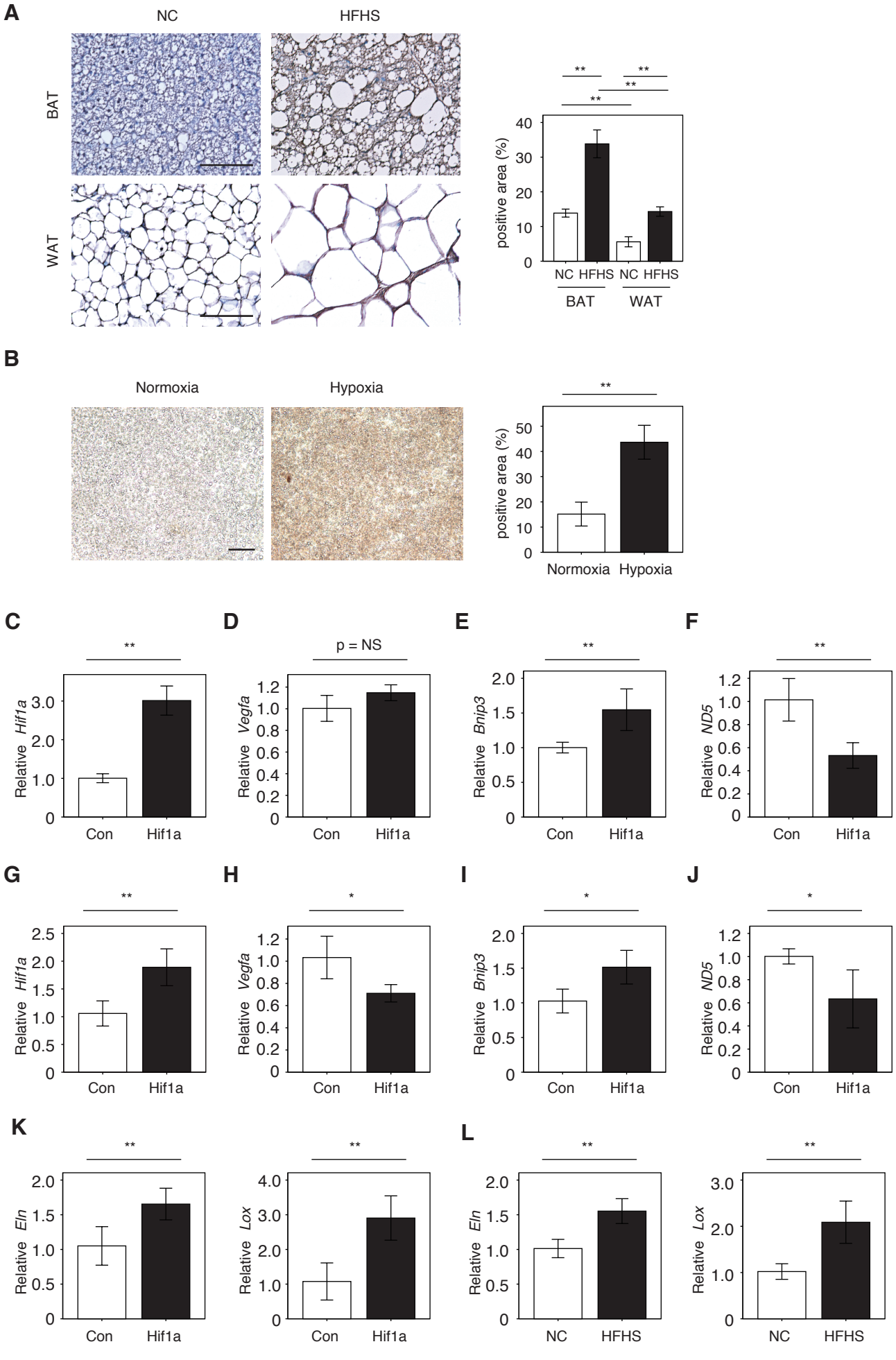

Supplemental Figure 11